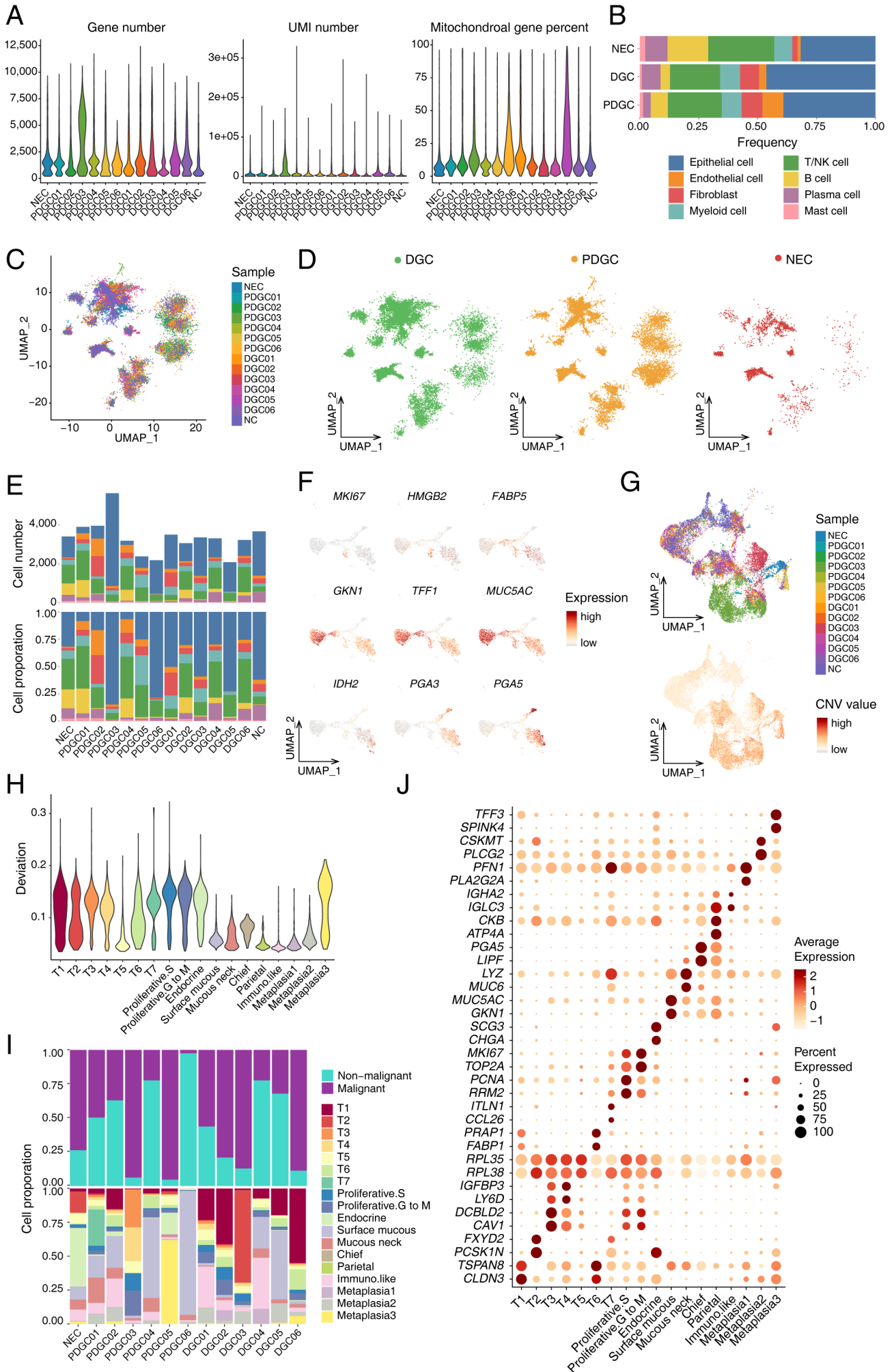


# Fig S1



**Figure S1.**

Representative single-cell transcriptome landscape of gastric cancer. **A** Violin plot showing detected gene number, transcripts number and mitochondrial gene percentage of each sample. **B** The distribution of all cell types in differentiated gastric cancer (DGC), poorly differentiated gastric cancer (PDGC) and neuroendocrine carcinoma (NEC). **C** Different sample sources information shown in UMAP plot (n = 46,883). **D** UMAP plot showing the distribution of cells from DGC, PDGC and NEC. **E** The cell number and proportion of different cell types in each sample. **F** UMAP plot showing the expression of different cell type markers in the normal mucosa tissue sample. **G** UMAP plot showing sample sources and CNV deviation information. **H** Violin plot showing CNV deviation of different epithelial cell clusters from non-malignant and malignant epithelial cells. **I** The percentage of malignant cells and different epithelial cell clusters in each sample. **J** The expression of corresponding markers for different epithelial cell clusters.

# Fig S2

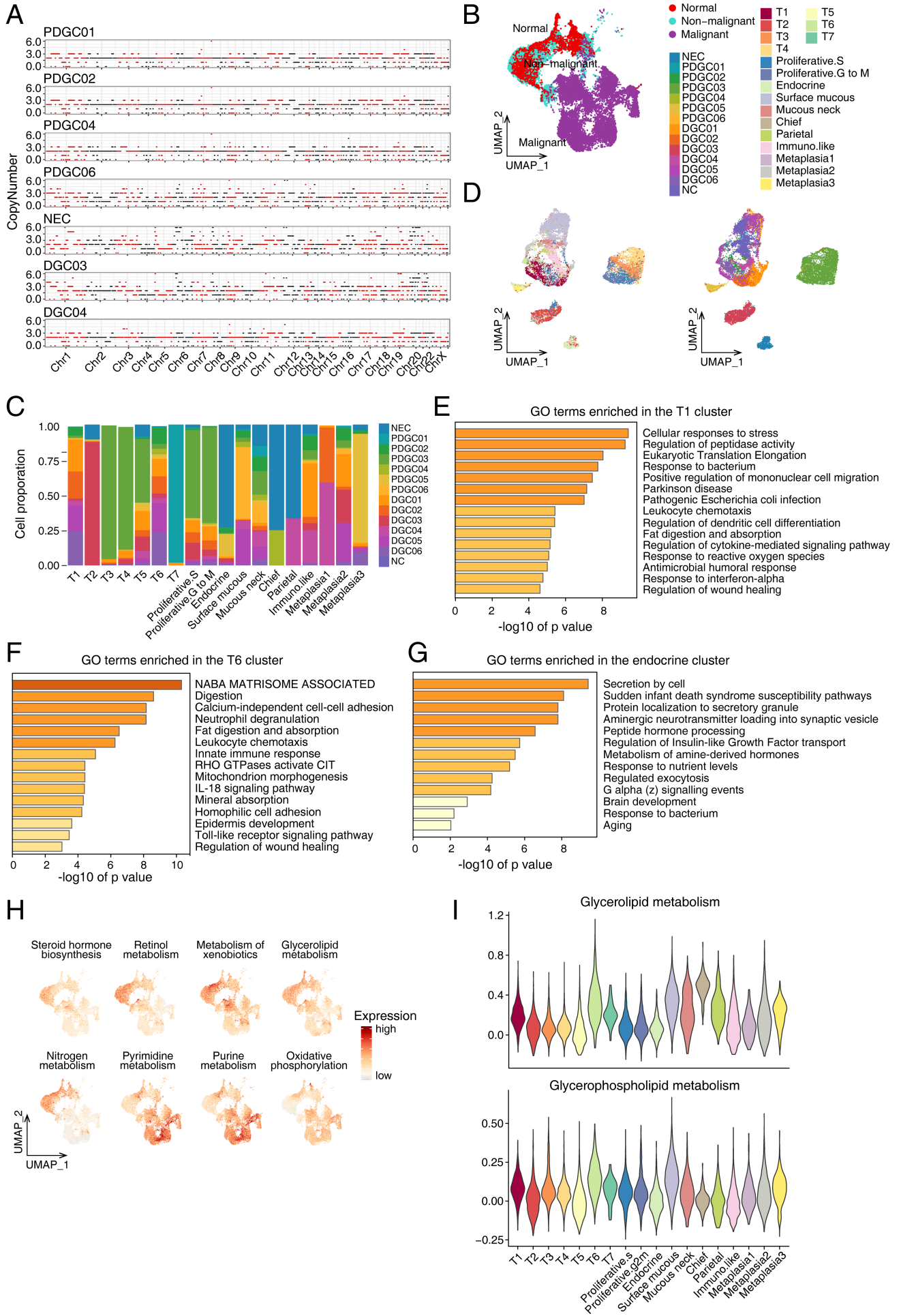


**Figure S2.**

Representative single-cell transcriptome landscape of gastric cancer. **A** Chromosomal landscape of large-scale copy number variations (CNV) inferred from whole exome sequencing data of the corresponding laser capture microdissected tissue. **B** UMAP plot showing normal, non-malignant and malignant epithelial cell clusters. **C** The percentage of cells from different sample in each cluster. **D** UMAP plot showing different epithelial cell clusters according to gene regulatory networks (GRNs). **E** Gene enrichment analysis showing the signaling pathways relatively up-regulated in T1 clusters. **F** Gene enrichment analysis showing the signaling pathways relatively up-regulated in T6 clusters. **G** Gene enrichment analysis showing the signaling pathways relatively up-regulated in endocrine clusters. **H** UMAP plot showing the metabolism-related activities in epithelial clusters. **I** Violin plot showing the expression levels of gene set signatures including glycerolipid metabolism and glycerophospholipid metabolism in different epithelial cell clusters.

# Fig S3

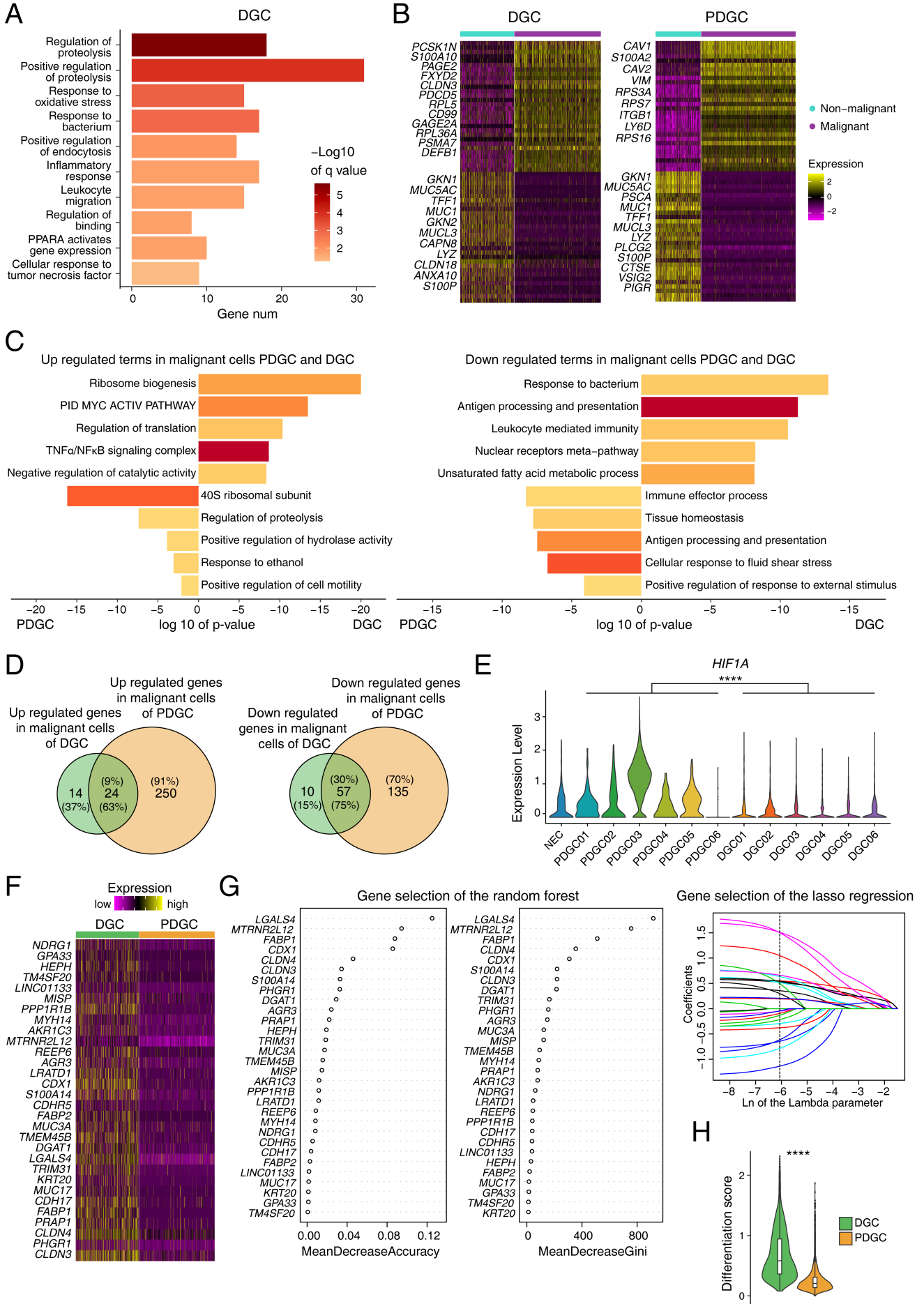


### Figure S3.

Comparison between differentiated gastric cancer (DGC) and poorly differentiated gastric cancer (PDGC). **A** Gene enrichment analysis showing the functions relatively up-regulated in DGC. **B** Heatmap showing differentially expressed genes (DEG) of PDGC and DGC compared with non-malignant epithelial cells. Part gene names are displayed. **C** Gene enrichment analysis showing the signaling pathways relatively up- or down-regulated in PDGC and DGC compared with non-malignant epithelial cells. **D** Venn diagram showing the number of up- and down-regulated genes in PDGC and DGC compared with non-malignant epithelial cells. **E** Violin plot showing the expression levels of *HIF1A* in different samples (\*\*\*\* - p value < 0.0001 calculated by wilcox test). **F** Heatmap showing the expression levels of genes which have the high correlation with DEGs of DGC compared to PDGC. **G** The processing of gene selection using the random forest and lasso regression methods. The left point plot showing the contributions of genes to the predicting output of DGC and PDGC. The right line plot showing the choices of the lambda values of the lasso regression. **H** Violin plot showing differentiation score in DGC and PDGC (\*\*\*\* - p value < 0.0001 calculated by wilcox test).

# Fig S4

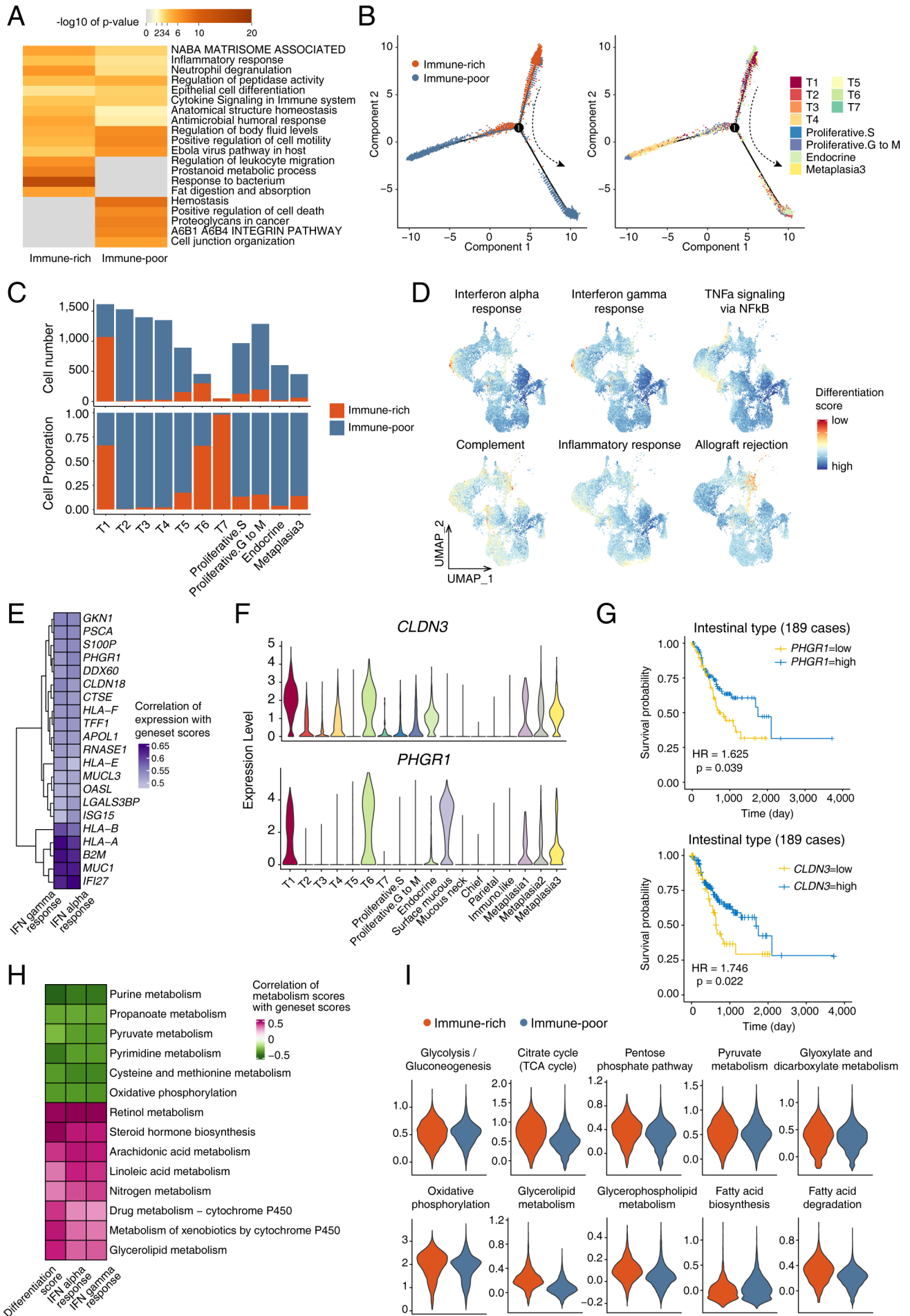


**Figure S4.**

Transcriptomic profiling of immune infiltration-related genes. **A** Gene enrichment analysis showing the signaling pathways relatively up- or down-regulated in immune-rich and immune-poor type gastric cancer. **B** Pseudotime trajectory of malignant epithelial cells according to the immune-related gene sets. **C** Number and percentage of immune-rich and immune-poor type cells in each malignant epithelial cluster. **D** UMAP plot showing expression of hallmark signatures and GO gene sets of immune response in epithelial cells. **E** Genes highly correlated with expression of interferon gamma and the interferon alpha pathways. **F** Violin plot showing expression levels of *PHGR1* and *CLDN3* in each epithelial cell cluster. **G** Kaplan-Meier survival curve showing the survival of intestinal-type gastric cancer cases in the TCGA dataset with high and low expression levels of *PHGR1* and *CLDN3*. **H** Metabolic activity-related gene sets highly correlated with expression of the differentiation gene set and interferon alpha/gamma response gene sets. **I** Violin plot showing expression levels metabolic activity-related gene sets in immune-rich and immune-poor type gastric cancer.

# Fig S5

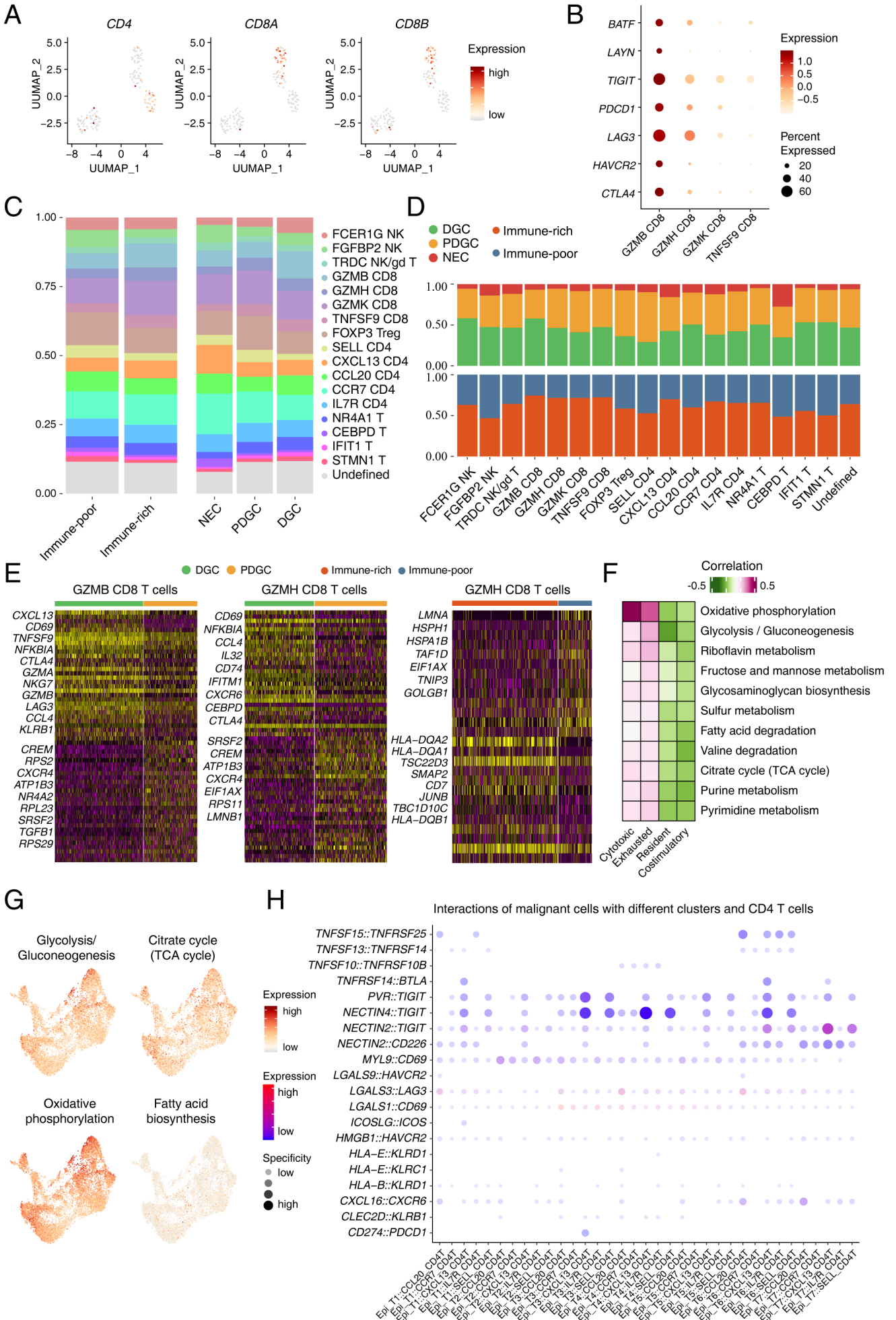


**Figure S5.**

Tumor infiltrating T cell characteristics and interactions with malignant cells. **A** UMAP plot showing expression of *CD4*, *CD8A* and *CD8B* in *STMNI*<sup>+</sup> T cells. **B** The expression of exhaustion-related genes in different types of CD8<sup>+</sup> T cells. **C** The percentage of different types of T cells in immune-rich and immune-poor type gastric cancer, and differentiated gastric cancer (DGC), poorly differentiated gastric cancer (PDGC) and neuroendocrine carcinoma (NEC). **D** The percentage of T cells from NEC, PDGC and NEC, and immune-rich and immune-poor type in different T cell clusters. **E** Heatmap showing differentially expressed genes between *GZMH*<sup>+</sup> CD8<sup>+</sup> T cells from immune-rich/poor type gastric cancer and DGC/PDGC, and between *GZMB*<sup>+</sup> CD8<sup>+</sup> T cells from DGC/PDGC. Part gene names are displayed. **F** Metabolic activity-related gene sets highly correlated with cytotoxic, exhausted, resident, costimulatory and cell cycle signatures of CD8<sup>+</sup> T cells. **G** UMAP plot showing expression of metabolic activity-related gene sets in T cells. **H** Interactions between epithelial cells and CD4<sup>+</sup> T cells inferred from cell communication analysis using toolkit NATMI.

# Fig S6

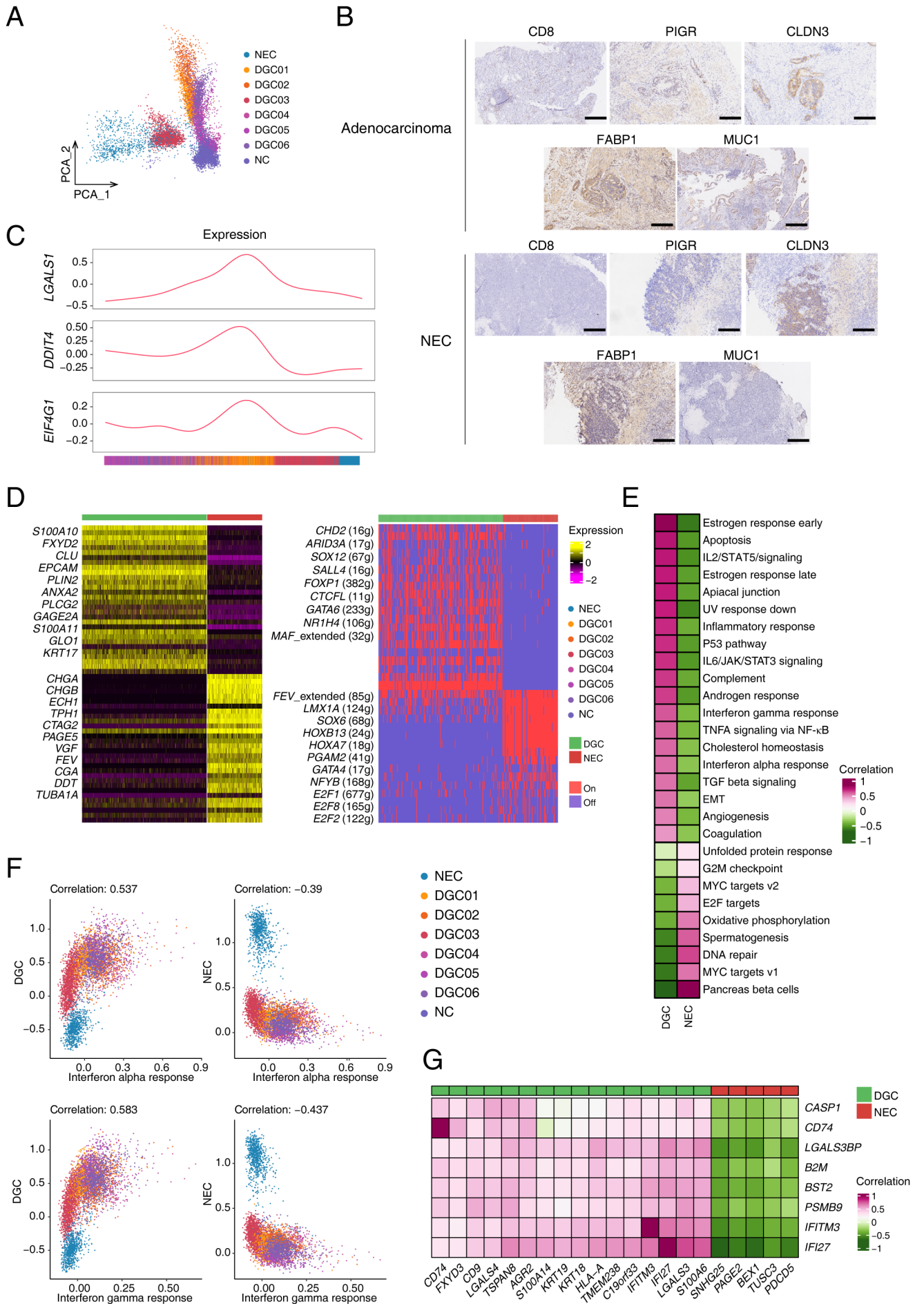


**Figure S6.**

Transition of differentiation status in mixed adenoneuroendocrine carcinoma. **A** PCA plot showing the distribution of epithelial cells from differentiated gastric adenocarcinoma (DGC), intermediate state (DGC01 and DGC03) and neuroendocrine carcinoma (NEC). **B** Representative images of immune-histochemical staining of CD8 and other differentially expressed proteins in adenocarcinoma and NEC components from the same mixed adenoneuroendocrine carcinoma. Scale bar, 300  $\mu\text{m}$ . **C** Representative genes that enriched in the intermediate state. **D** Heatmap showing differentially expressed genes between DGC and NEC and gene regulatory networks that changed gradually along the trans-differentiation path of DGC to NEC. Part gene and TF names are displayed. **E** Hallmark gene signatures highly correlated with DGC and NEC. **F** The correlation between interferon alpha/gamma response genes and DGC, intermediate state (DGC01 and DGC03) and NEC. **G** The correlation between specific genes in interferon-related pathways and DGC/NEC.